

## (Supporting Information)

### Reactivity of Amido Ligands on a Dinuclear Ru(II) Center: Formation of Imido Complexes and C–N Coupling Reaction with Alkyne

Shin Takemoto, Tomoharu Kobayashi, and Hiroyuki Matsuzaka<sup>\*</sup>

Department of Chemistry, Faculty of Arts and Sciences, Osaka Prefecture University, Sakai, Osaka 599-8531, Japan and Coordination Chemistry Laboratories, Institute for Molecular Science, Myodaiji, Okazaki 444-8585, Japan

#### Contents

<b>Experimental Procedure</b>	S2
<b>Table S1.</b> Crystallographic Data for <b>3</b> , <b>4</b> , <b>5</b> , and <b>6</b> .	S6
<b>Figure S1.</b> ORTEP drawing of <b>3</b> .	S8
<b>Figure S2.</b> ORTEP drawing of <b>4</b> .	S9
<b>Figure S3.</b> ORTEP drawing of <b>5</b> .	S10
<b>Figure S4.</b> ORTEP drawing of <b>6</b> .	S11
<b>Computational Details</b>	S12
<b>Table S2.</b> Selected bond lengths and angles in optimized geometries.	S12
<b>Figure S5.</b> MO diagram of [(CpRu) <sub>2</sub> (μ <sub>2</sub> -NH)(μ <sub>2</sub> -CO)] ( <b>3'</b> ).	S13
<b>Figure S6.</b> Occupied molecular orbitals of <b>3'</b> .	S14

## Experimental Procedure

**General.** All manipulations were carried out under an atmosphere of dinitrogen using standard Schlenk-line techniques. Solvents were dried and distilled over an appropriate drying agent under an atmosphere of dinitrogen.  $[\text{Cp}^*\text{RuCl}]_4$  was prepared according to the literature.<sup>1</sup> All commercially available reagents were used as received. NMR spectra were recorded on a JEOL ECP500 spectrometer. Infrared spectra were recorded on a Hitachi Nicolet I-5040 FT-IR spectrometer. Elemental analyses were performed using a Perkin Elmer CHNS series II microanalyzer.

**$[(\text{Cp}^*\text{Ru})(\mu_2\text{-NHPh})_2]$  (**1**).** This complex was prepared by a slightly modified method of Don Tilley et al.<sup>2</sup> A solution of *n*-BuLi in *n*-hexane (2.64 M, 500  $\mu\text{L}$ , 1.32 mmol) was added to a solution of aniline (100  $\mu\text{L}$ , 1.10 mmol) in THF (15 mL) at  $-80^\circ\text{C}$  and the mixture was stirred at  $-80^\circ\text{C}$  for 0.5 h. To this solution was added  $[\text{Cp}^*\text{RuCl}]_4$  (299 mg, 0.275 mmol) and the reaction mixture was allowed to warm to room temperature with stirring over 12 h to form a dark blue solution. The solvents were removed in vacuo and the residue was extracted with hexanes (15 mL). Evaporation of hexanes gave **1** as a dark blue solid (250 mg, 69%), which was pure as judged by  $^1\text{H}$  NMR spectroscopy and used for subsequent reactions.

**$[(\text{Cp}^*\text{Ru})_2(\mu_2\text{-CO})(\mu_2\text{-NPh})]$  (**3**).** To a solution of **1** (210 mg, 0.320 mmol) in THF (15 mL) was added CO (11 mL, 0.5 mmol) at room temperature. The color of the solution rapidly changed from blue to yellow. After stirring overnight at room temperature, the solvent was removed in vacuo and the remaining solid was extracted with hexanes (30 mL). The hexanes solution was concentrated to 10 mL and stand overnight. Red crystals were collected by filtration and then dried in vacuo furnishing 120 mg (63%) of **3**. Anal. Calcd for  $\text{C}_{27}\text{H}_{35}\text{NORu}_2$ : C, 54.81; H, 5.96; N, 2.37. Found: C, 54.87; H, 5.95; N, 2.33.  $^1\text{H}$  NMR (500 MHz,  $\text{C}_6\text{D}_6$ ):  $\delta$  7.38 (m, 2H), 7.16 (m, 1H), 7.12 (m, 2H), 1.63 (s, 30H,  $\text{Cp}^*$ ).  $^{13}\text{C}\{^1\text{H}\}$  NMR (100.40 MHz, toluene- $d_8$ ,  $22^\circ\text{C}$ ):  $\delta$  258.7 (s,  $\mu_2\text{-CO}$ ), 168.5, 122.1, 117.6 (s, Ph), 91.0 ( $\text{C}_5\text{Me}_5$ ), 9.8 ( $\text{C}_5\text{Me}_5$ ). IR (KBr):  $1744\text{ cm}^{-1}$  ( $\nu(\text{CO})$ ).

**Observation of  $[(\text{Cp}^*\text{Ru})_2(\mu_2\text{-CO})(\mu_2\text{-NHPPh})_2]$  (**2**).** To a solution of **1** (60 mg, 0.091 mmol) and ferrocene (9 mg, 0.048 mmol) as an internal standard in  $\text{C}_6\text{D}_6$  (2 mL) was added CO (2 mL, 0.09 mmol) at room temperature. The  $^1\text{H}$  NMR spectrum measured after 15 min showed the formation of **2** (84%), **3** (14%), and  $[\text{Cp}^*\text{Ru}(\text{CO})_2]_2$  (2%).  $^1\text{H}$  NMR data for **2** (500 MHz,  $\text{C}_6\text{D}_6$ ):  $\delta$  7.12, 6.93, 6.84, 6.69, 6.55 (m, 2H each), 1.45 (s, 30H,  $\text{Cp}^*$ ), 0.40 (s, 2H, NH). IR data for **2** (KBr):  $1775\text{ cm}^{-1}$  ( $\nu(\text{CO})$ ).  $^{13}\text{C}\{^1\text{H}\}$  NMR data for **2** (100.40 MHz, toluene- $d_8$ ,  $-49\text{ }^\circ\text{C}$ ):  $\delta$  249.6 (s,  $\mu_2\text{-CO}$ ), 159.4, 125.0, 119.6, 117.9, 116.8, 114.3 (s, Ph), 87.4 ( $\text{C}_5\text{Me}_5$ ), 8.5 ( $\text{C}_5\text{Me}_5$ ). MS (FAB):  $m/z$  685  $[\text{M}-\text{H}]^+$ .

**$[(\text{Cp}^*\text{Ru})_2(\mu_2\text{-}t\text{-BuNC})(\mu_2\text{-NPh})]$  (**4**).** To a solution of **1** (158 mg, 0.241 mmol) in THF (10 mL) was added  $t\text{-BuNC}$  (27.3  $\mu\text{L}$ , 0.241 mmol) at room temperature. The dark brown solution was stirred overnight at room temperature, and evaporated to dryness. Recrystallization of the residue from toluene–hexanes (2 mL/10 mL) afforded dark red crystals of **4** (30 mg). The mother liquor was evaporated to dryness, and the residue was recrystallized from toluene–hexanes (1 mL/5 mL) to give the second crop of the crystals (33 mg). Combined yield 63 mg, 40%.  $^1\text{H}$  NMR (500 MHz,  $\text{C}_6\text{D}_6$ ):  $\delta$  7.38 (m, 2H), 7.13 (m, 1H), 7.01 (m, 2H), 1.97 (s, 9H,  $t\text{-Bu}$ ), 1.56 (s, 30H,  $\text{Cp}^*$ ). IR (KBr):  $1809\text{ cm}^{-1}$  ( $\nu(\text{CN})$ ). Satisfactory combustion data could not be obtained under our elemental analysis conditions, presumably due to the extreme sensitivity of **4** to dioxygen.

**$[(\text{Cp}^*\text{Ru})_2(\mu_2\text{-CH}_2)(\mu_2\text{-NPh})]$  (**5**).** To a stirred suspension of  $[\text{Ph}_2\text{MeS}][\text{BF}_4]$  (211 mg, 0.734 mmol) in THF (10 mL) was added dropwise a solution of  $\text{NaN}(\text{SiMe}_3)_2$  in THF (1.0 M, 807  $\mu\text{L}$ ) at  $-78\text{ }^\circ\text{C}$ . The mixture was slowly warmed to  $-10\text{ }^\circ\text{C}$  to form a clear yellow solution. The solution was cooled again to  $-78\text{ }^\circ\text{C}$  and then transferred via cannula to a Schlenk flask containing a THF (20 mL) solution of **1** (482 mg, 0.734 mmol) that was also cooled to  $-78\text{ }^\circ\text{C}$ . The combined solution was allowed to warm to room temperature with stirring over 12 h. The solvent was removed in vacuo and

the residue was extracted with toluene (20 mL). The toluene solution was evaporated to dryness and the residue was washed with 5 mL of hexanes. The remaining solid was recrystallized from toluene–hexanes (2 mL/10 mL) to give **5** as dark red crystals. Yield 345 mg, 81%. Anal. Calcd for  $C_{27}H_{37}NRu_2$ : C, 56.13; H, 6.46; N, 2.42. Found: C, 55.97; H, 6.36; N, 2.84.  $^1H$  NMR (500 MHz,  $C_6D_6$ ):  $\delta$  12.79 (s, 2H,  $CH_2$ ), 7.36 (m, 3H), 7.14 (m, 2H), 1.63 (s, 30H, Cp\*).  $^{13}C\{^1H\}$  NMR (125.6 MHz,  $C_6D_6$ ):  $\delta$  186.61 (s,  $CH_2$ ), 168.91 (s, Ph), 136.42 (s, Ph), 131.35 (s, Ph), 120.32 (s, Ph), 86.06 (s,  $C_3Me_5$ ), 10.72 (s,  $C_3Me_5$ ).

**$[(Cp^*Ru)_2(\mu_2-\eta^3:\eta^3-PhNCPhCPh)]$  (**6**).** To a solution of **1** (352 mg, 0.536 mmol) in THF (20 mL) was added diphenylacetylene (95.5 mg, 0.536 mmol) at room temperature, and the dark brown solution was stirred overnight at room temperature. The solvent was removed in vacuo, and the residue was recrystallized from toluene–hexanes (2 mL/10 mL) to give **6** as dark red crystals. Yield 210 mg, 53%. Anal. Calcd for  $C_{40}H_{45}NRu_2$ : C, 64.75; H, 6.11; N, 1.89. Found: C, 64.55; H, 6.22; N, 1.80.  $^1H$  NMR (500 MHz,  $C_6D_6$ ):  $\delta$  7.68 (m, 4H), 7.34 (m, 2H), 7.22 (m, 2H), 7.14 (m, 1H), 7.02 (m, 1H), 6.90 (m, 3H), 6.65 (m, 2H), 1.66 (s, 30H, Cp\*).

**X-ray Crystallography.** Crystallographic data are summarized in Table S1. A single crystal suitable for X-ray crystallography was sealed in a glass capillary. All measurements were performed on a Rigaku RAXIS Rapid diffractometer equipped with an imaging plate detector. The frame data were processed using the Rigaku PROCESS-AUTO program,<sup>3</sup> and the reflection data were corrected for absorption with an ABSCOR program.<sup>4</sup>

The structures were solved by direct method and refined on  $F^2$  by full-matrix least-squares method by using SHELX97.<sup>5</sup> Anisotropic refinement was applied to all non hydrogen atoms. Hydrogen atoms were located at the calculated positions and treated as riding models.

Two types of severe disorders were found for the *t*-butyl isocyanide ligand in **4**. One arises from the two independent orientations of the *t*-Bu group, and the other is due to the presence of two distinct

C(7)–N–C(8) linkages (Figure S2). Two pairs of three methyl carbon atoms were placed on the central *t*-Bu carbon atom (C(8)) and allowed to have split occupancies (60% and 40%). Similarly, the isocyanide nitrogen atom was divided into two nitrogen atoms with 65% and 35% site occupancies. The disordered atoms were isotropically refined, and no hydrogen atoms were placed on the *t*-Bu carbon atoms.

**Table S1. Crystallographic data for 3, 4, 5, and 6.**

	<b>3</b>	<b>4</b>
formula	$C_{27}H_{35}NORu_2$	$C_{31}H_{44}N_2Ru_2$
<i>M</i>	591.70	646.82
<i>T</i> /K	296	296
crystal size (mm)	0.30 × 0.30 × 0.10	0.30 × 0.30 × 0.10
crystal system	triclinic	monoclinic
space group	<i>P</i> 1	<i>P</i> 2 <sub>1</sub> / <i>c</i>
<i>Z</i>	2	4
<i>a</i> (Å)	8.616(2)	10.4556(7)
<i>b</i> (Å)	10.869(3)	20.399(3)
<i>c</i> (Å)	15.068(4)	14.3790(14)
<i>α</i> (deg)	102.086(9)	90
<i>β</i> (deg)	94.544(11)	104.395(5)
<i>γ</i> (deg)	111.186(11)	90
<i>V</i> (Å <sup>3</sup> )	1268.8(6)	2970.5(6)
<i>D</i> <sub>calc</sub> (g/cm <sup>3</sup> )	1.550	1.446
<i>μ</i> (Mo-Kα) (mm <sup>-1</sup> )	1.209	1.037
reflections collected	12489	25536
unique reflections	5791	6690
GOF on F <sup>2</sup>	0.925	1.052
R1 [ <i>I</i> > 2σ( <i>I</i> )] <sup>a</sup>	0.0599	0.0485
wR2 (all data) <sup>b</sup>	0.1295	0.1241

$$^a R1 = \sum ||Fo| - |Fc|| / \sum |Fo|, \quad ^b wR2 = [\sum (w(Fo^2 - Fc^2)^2) / \sum w(Fo^2)^2]^{1/2}$$

**Table S1. Crystallographic data for 3, 4, 5, and 6 (continued).**

	<b>5</b>	<b>6</b>
formula	$C_{27}H_{37}NRu_2$	$C_{40}H_{45}NRu_2$
<i>M</i>	577.72	741.91
<i>T</i> /K	296	296
crystal size (mm)	0.50 × 0.40 × 0.10	0.50 × 0.40 × 0.10
crystal system	triclinic	orthorhombic
space group	<i>P</i> 1	<i>Pbcn</i>
<i>Z</i>	2	4
<i>a</i> (Å)	8.621(3)	16.2289(14)
<i>b</i> (Å)	11.041(4)	12.5086(13)
<i>c</i> (Å)	15.143(6)	17.0085(11)
$\alpha$ (deg)	103.82(3)	90
$\beta$ (deg)	89.08(3)	90
$\gamma$ (deg)	113.05(3)	90
<i>V</i> (Å <sup>3</sup> )	1282.9(8)	3452.7(5)
<i>D</i> <sub>calc</sub> (g/cm <sup>3</sup> )	1.496	1.427
$\mu$ (Mo-K $\alpha$ ) (mm <sup>-1</sup> )	1.190	0.902
reflections collected	12553	29986
unique reflections	5796	3894
GOF on <i>F</i> <sup>2</sup>	0.996	0.999
R1 [ <i>I</i> > 2 $\sigma$ ( <i>I</i> )] <sup>a</sup>	0.0552	0.0436
wR2 (all data) <sup>b</sup>	0.1222	0.1015

<sup>a</sup>  $R1 = \sum ||Fo| - |Fc|| / \sum |Fo|$ , <sup>b</sup>  $wR2 = [\sum (w(Fo^2 - Fc^2)^2) / \sum w(Fo^2)^2]^{1/2}$

**Figure S1.** ORTEP drawing of **3**.

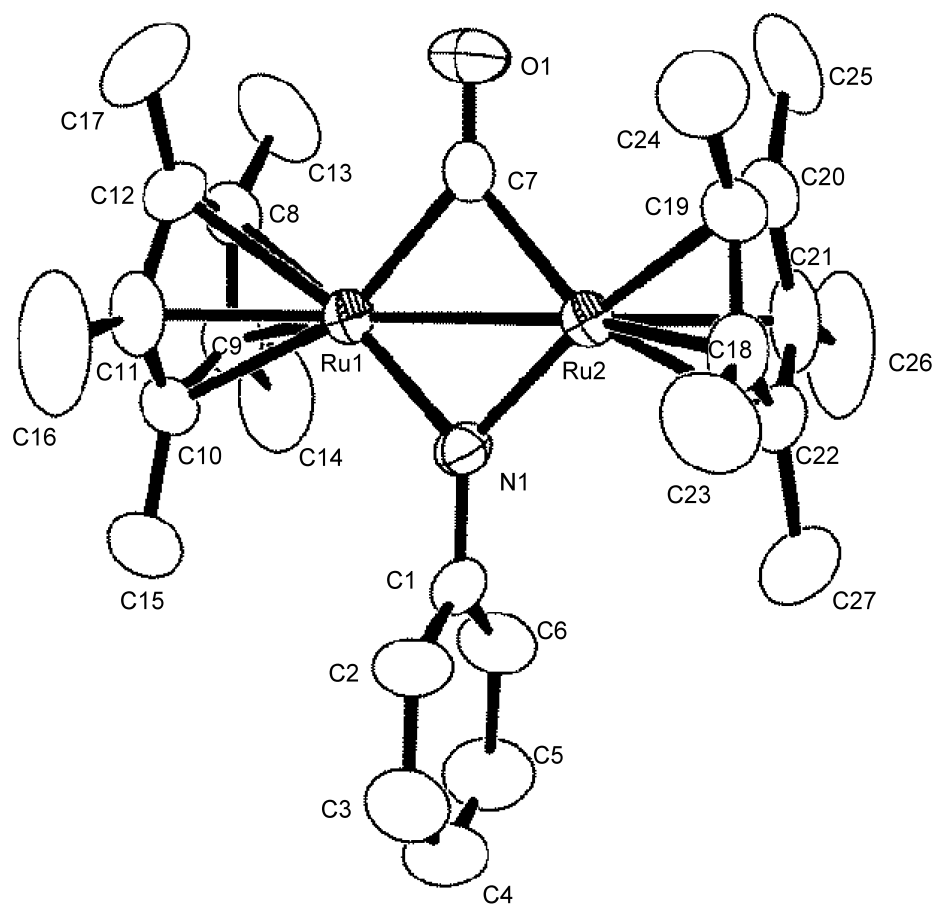




**Figure S2.** ORTEP drawing of 4.

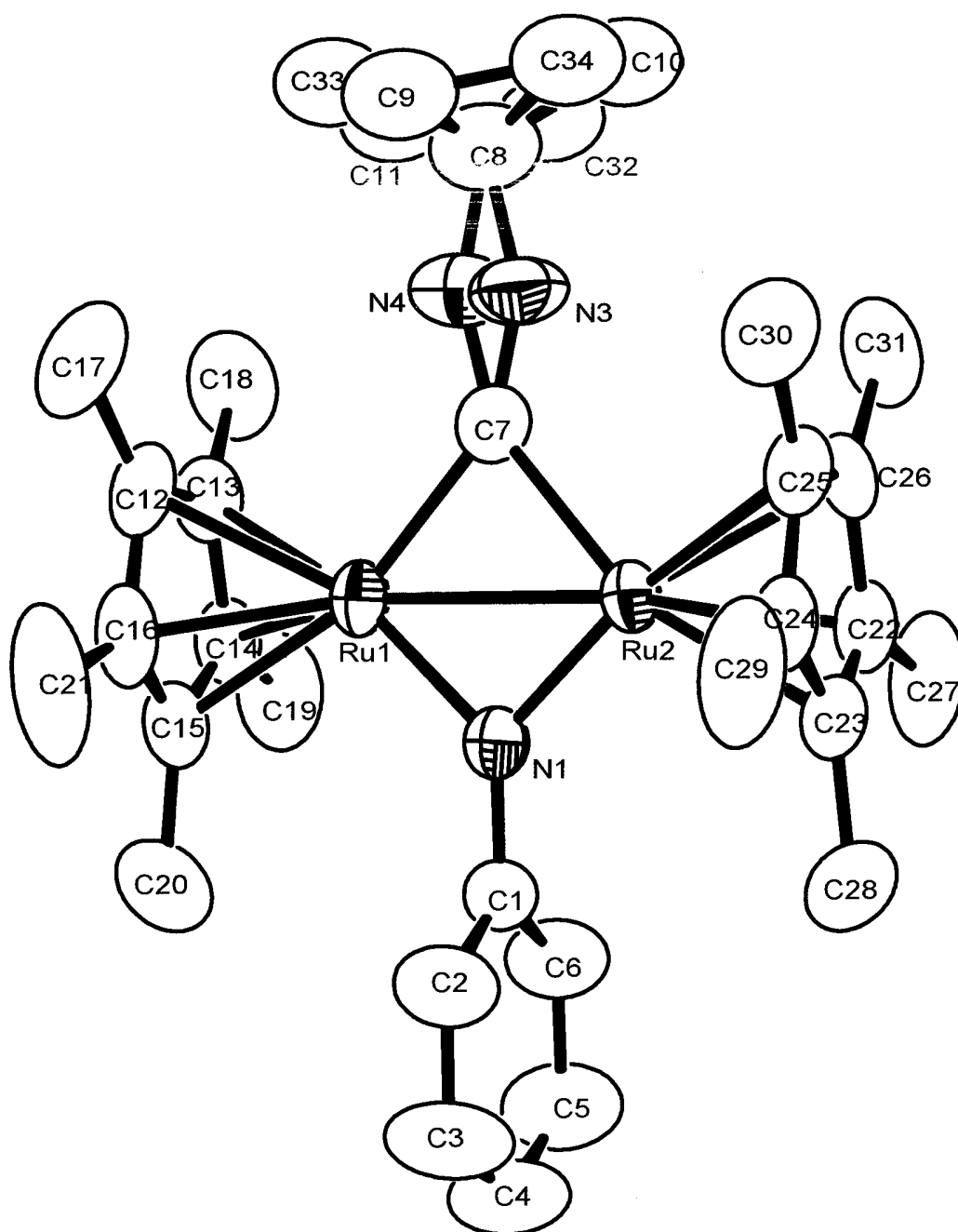


**Figure S3.** ORTEP drawing of **5**.

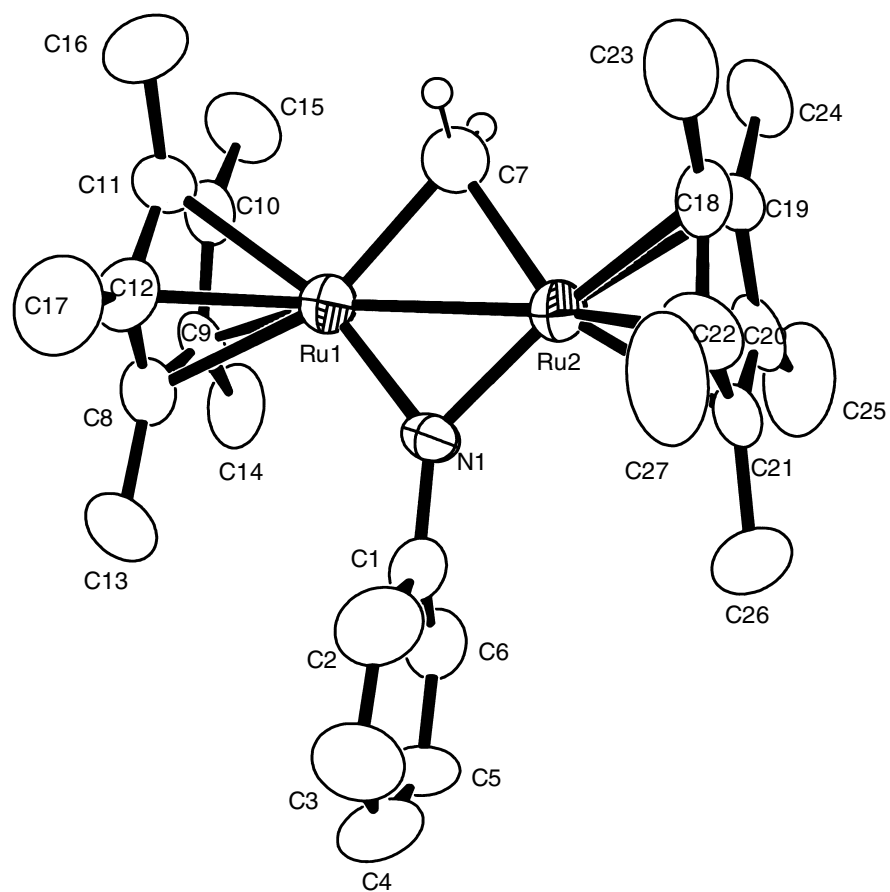
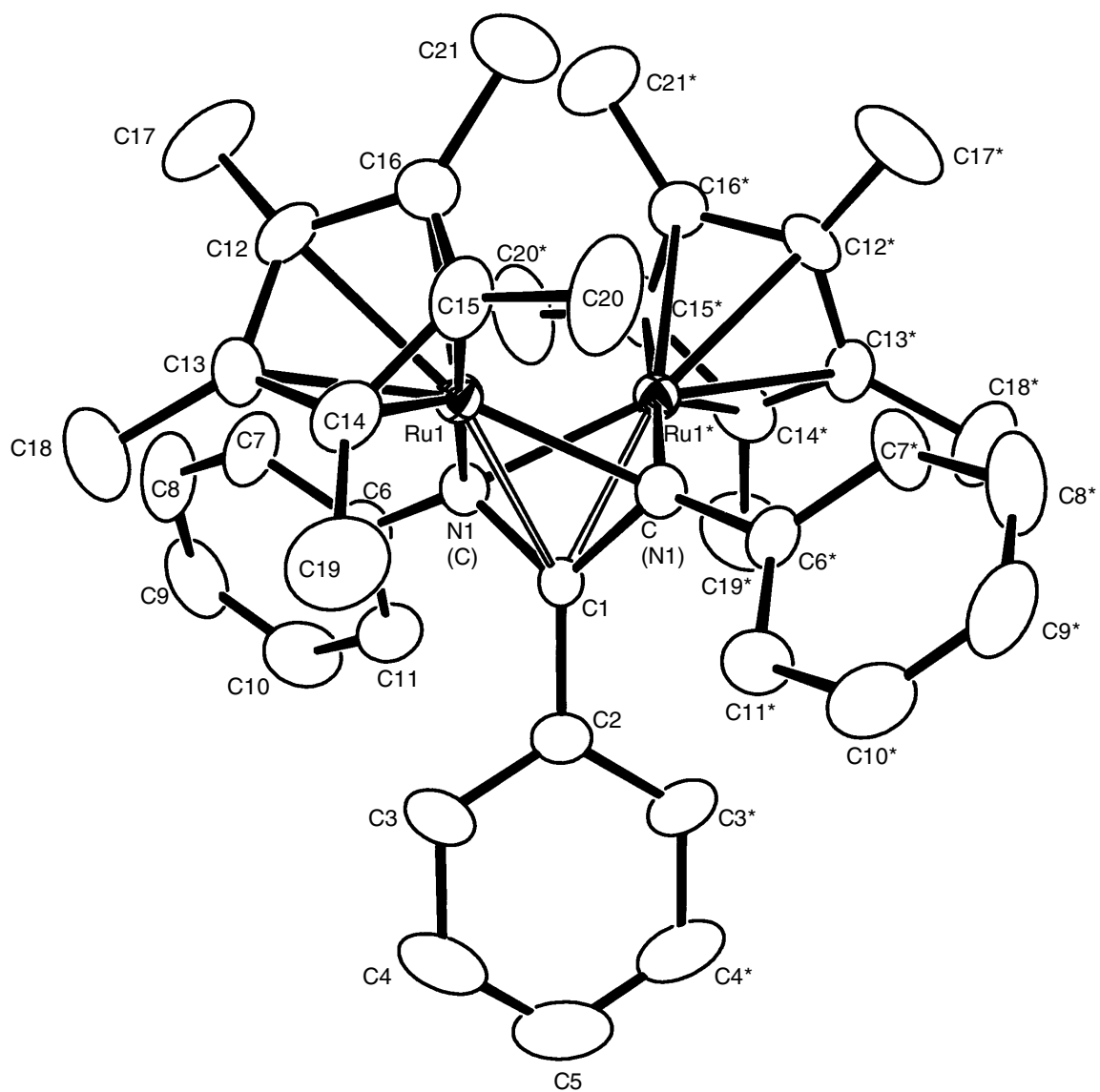


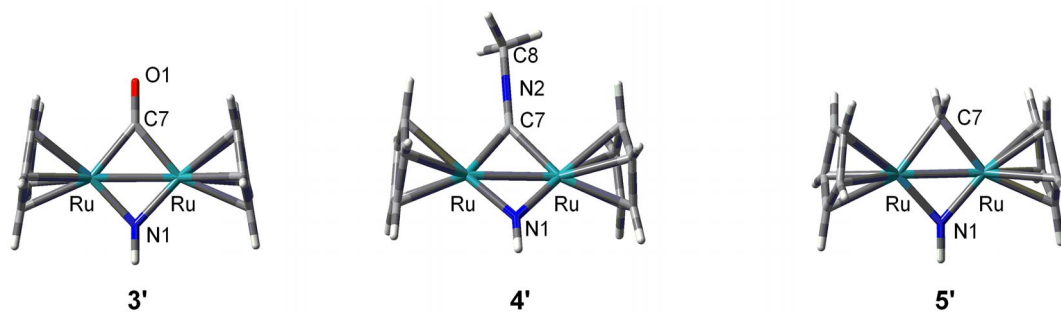
**Figure S4.** ORTEP drawing of **6**.



## Computational Studies

**Method.** Electronic structures of the imido complexes **3–5** were studied by employing model complexes  $[(\text{CpRu})_2(\mu_2\text{-NH})(\mu_2\text{-L})]$  ( $\text{L} = \text{CO}$  (**3'**),  $\text{CNMe}$  (**4'**), and  $\text{CH}_2$  (**5'**)). All calculations were performed by DFT methods as implemented in the Gaussian03 program package.<sup>6</sup> Geometries of the model complexes were optimized by employment of a Becke-type three-parameter density functional model B3PW91 with LANL2DZ basis set.<sup>7,8</sup>  $C_{2v}$  symmetry was assumed for complexes **3'** and **5'**, and  $C_s$  symmetry for complex **4'**. Selected structural parameters for the optimized structures are listed in Table S2. A qualitative molecular orbital diagram showing the formation of **3'** from  $[\text{CpRuRuCp}]^{2+}$ , CO, and  $\text{NH}^{2-}$  fragments is shown in Figure S5, and the pictures of the selected occupied molecular orbitals of **3'** are provided in Figure S6.

**Table S2.** Selected bond lengths (Å) and angles (deg) in the optimized structures. Corresponding distances and angles obtained by X-ray studies of **3–5** were included for comparison.



	<b>3'</b>		<b>4'</b>		<b>5'</b>	
	DFT	X-ray	DFT	X-ray	DFT	X-ray
Ru–Ru	2.6296	2.6013(9)	2.6675	2.6594(5)	2.5987	2.5728(11)
Ru–N1	1.893	1.876(6)	1.889	1.890(4)	1.898	1.894(5)
		1.880(6)		1.885(4)		1.891(5)
Ru–C7	2.018	2.002(8)	2.074	2.090(5)	2.054	2.057(6)
		1.993(8)		2.082(5)		2.061(6)
C7–O1	1.212	1.201(9)				
C7–Ru–N1	95.361	95.4(3)	95.058	95.40(18)	97.559	98.6(2)
		95.6(3)		95.81(19)		98.4(2)
Ru–N1–Ru	87.987	87.7(2)	89.839	89.57(18)	86.420	85.64(19)

Ru-C7-Ru	81.291	81.3(3)	80.049	79.20(19)	78.462	77.3(2)
----------	--------	---------	--------	-----------	--------	---------

**Figure S5.** MO diagram of  $[(\text{CpRu})_2(\mu_2\text{-NH})(\mu_2\text{-CO})]$  (**3'**). Cp-based orbitals are not included.

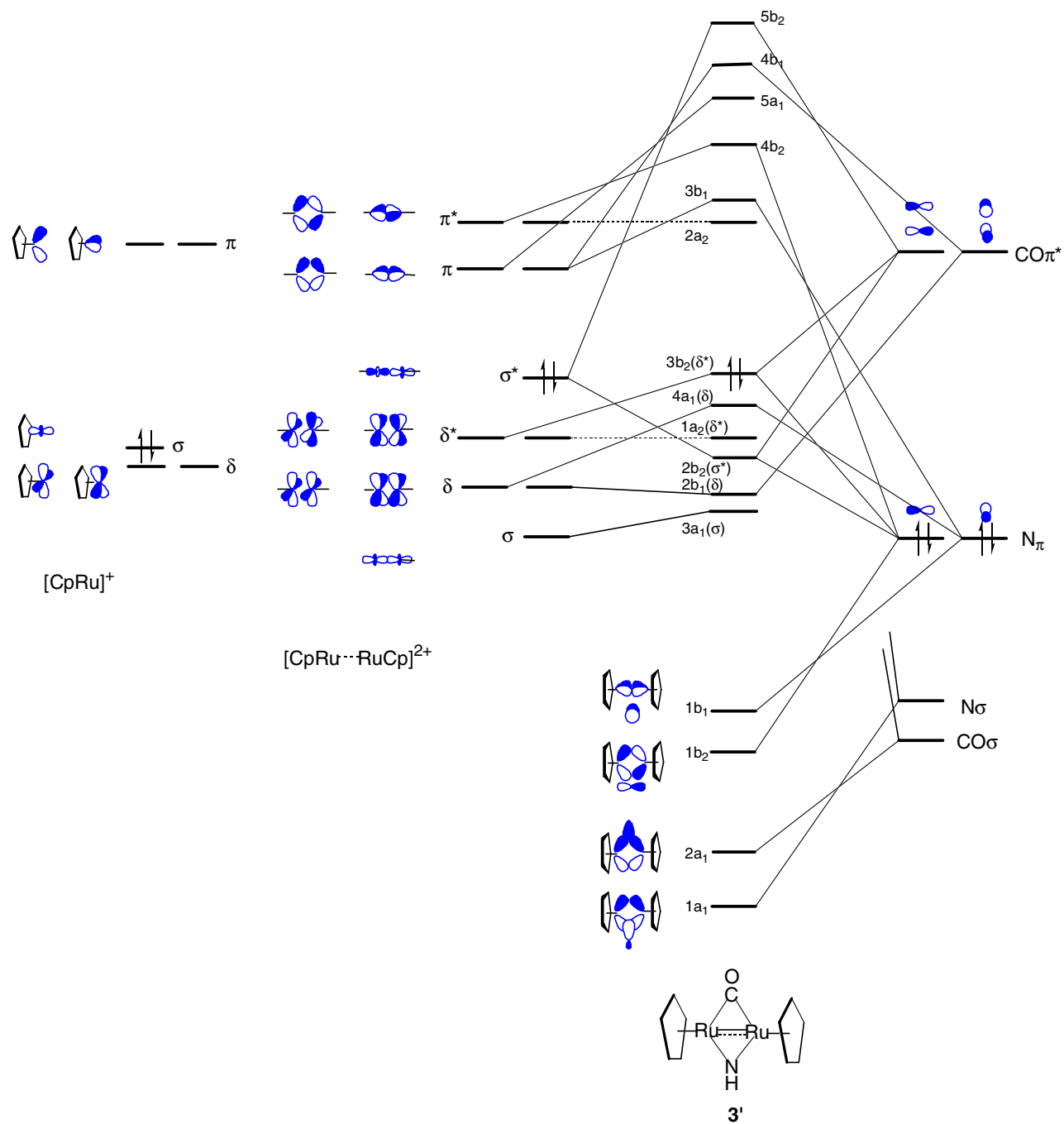
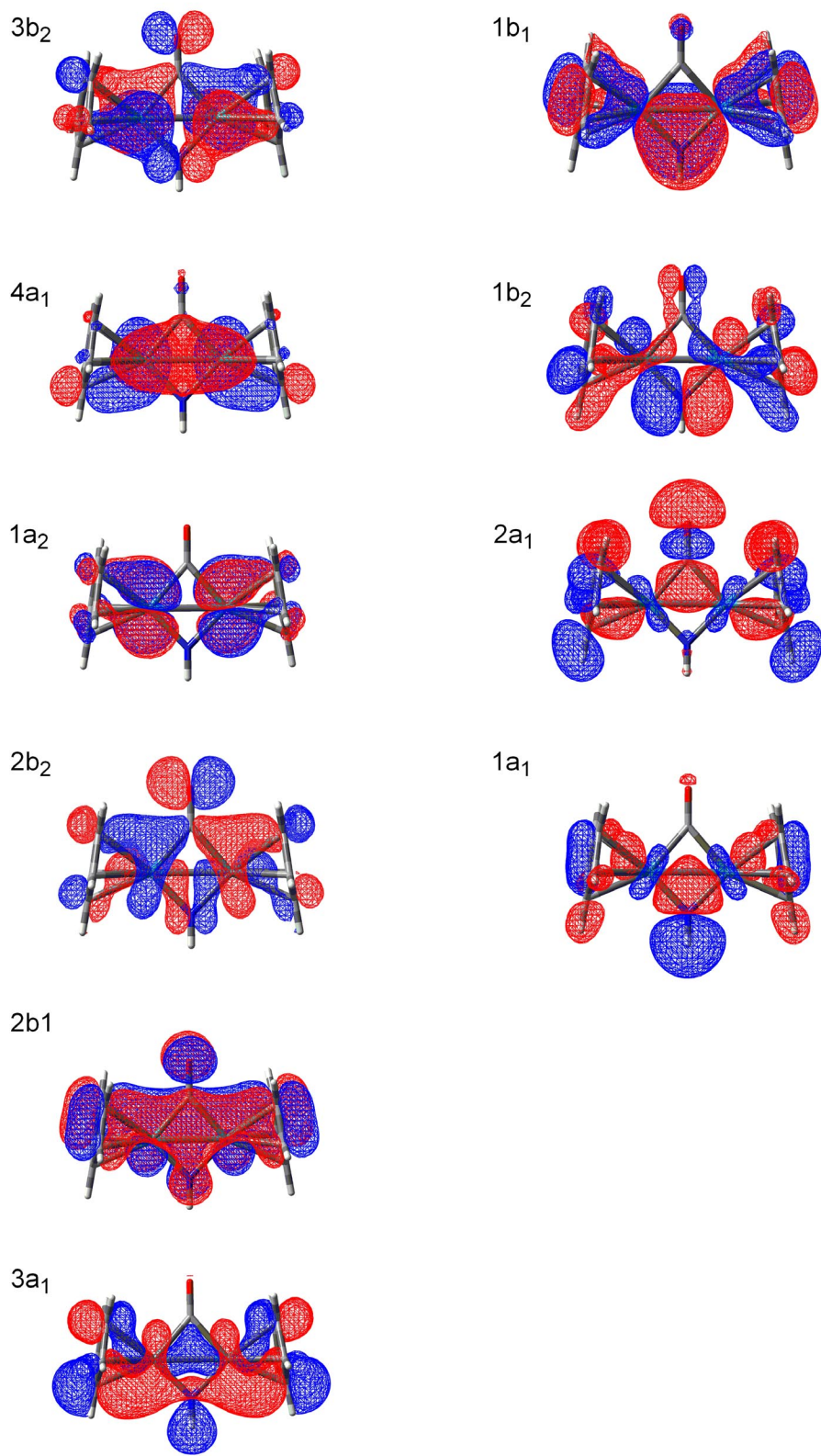


**Figure S6.** Selected occupied molecular orbitals of **3'**.



## References

- (1) Fagan, P. J.; Ward, M. D.; Calabrese, J. C. *J. Am. Chem. Soc.* **1989**, *111*, 1698.
- (2) Blake, R. E., Jr.; Heyn, R. H.; Tilley, T. D. *Polyhedron* **1992**, *11*, 709.
- (3) *PROCESS-AUTO, Automatic Data Acquisition and Processing Package for Imaging Plate Diffractometer*; Rigaku Corporation: Tokyo, Japan, 1998.
- (4) Higashi, T. *ABSCOR, Empirical Absorption Correction based on Fourier Series Approximation*; Rigaku Corporation: Tokyo, Japan, 1995.
- (5) Sheldrick, G. M. *SHELX97, Program for Crystal Structure Determination*; University of Göttingen: Göttingen, Germany, 1997.
- (6) Frisch, M. J.; Trucks, G. W.; Schlegel, H. B.; Scuseria, G. E.; Robb, M. A.; Cheeseman, J. R.; Zakrzewski, V. G.; Montgomery, J. A., Jr.; Stratmann, R. E.; Burant, J. C.; Dapprich, S.; Millam, J. M.; Daniels, A. D.; Kudin, K. N.; Strain, M. C.; Farkas, O.; Tomasi, J.; Barone, V.; Cossi, M.; Cammi, R.; Mennucci, B.; Pomeli, C.; Adamo, C.; Clifford, S.; Ochterski, J.; Petersson, G. A.; Ayala, P. Y.; Cui, Q.; Morokuma, K.; Malick, D. K.; Rabuck, A. D.; Raghavachari, K.; Foresman, J. B.; Ciolowski, J.; Ortiz, J. V.; Baboul, A. G.; Stefanov, B. B.; Liu, G.; Liashenko, A.; Piskorz, P.; Koramomi, I.; Gomperts, R.; Martin, R. L.; Fox, D. J.; Keith, T.; Al-Laham, M. A.; Peng, C. Y.; Nanayakkara, A.; Gonzalez, C.; Challacombe, M.; Gill, P. M. W.; Johnson, B.; Chen, W.; Wong, M. W.; Andres, J. L.; Head-Gordon, M.; Replogle, E. S.; Pople, J. A. *Gaussian 03*, Revision A.1; Gaussian, Inc., Pittsburgh, PA, 2003.
- (7) (a) Becke, A. D. *J. Chem. Phys.* **1993**, *98*, 5648. (b) Perdew, J. P.; Wang, Y. *Phys. Rev.* **1992**, *B45*, 13244.
- (8) Wadt, W. R.; Hay, P. J. *J. Chem. Phys.* **1985**, *82*, 284.
- (9) Orbital diagram of the  $[\text{CpRu}\cdots\text{RuCp}]^{2+}$  fragment has been described by several authors: Loren, S. D.; Campion, B. K.; Hein, R. H.; Tilley, T. D.; Bursten, B. E.; Luth, K. W. *J. Am. Chem. Soc.* **1989**, *111*, 4712–4718. See also, Burdett, J. K.; Albright, T. A.; Whangbo, M.-H. *Orbital Interactions in Chemistry*; Wiley: New York, 1985; Chapter 20.